ORIGINAL PAPER

Formulation of Cabotegravir Loaded Gold Nanoparticles: Optimization, Characterization to In-Vitro Cytotoxicity Study

Purnima Rawat[1] · Syed Sarim Imam[2] · Sharad Gupta[1]

Abstract

The effective and preventive treatment of HIV is one of the difficult challenges worldwide. It requires the development of an effective prophylactic strategy to prevent HIV/AIDS. This study aimed to synthesize Cabotegravir (CAB)-biodegradable gold (Au) nanoparticles by using pectin as a reducer and stabilizer. CAB-GNPs were prepared by the slightly modified *Turkevich* method. CAB-GNPs were optimized using Box Behnken design for independent variables gold chloride (A), pectin (B) and pH range (C). The effects of independent variables were observed on particle size (Y^1) and encapsulation efficiency (Y^2). The results of the study revealed that the optimized nanoparticles (GLN7) had a particle size of 3.9 ± 0.1 nm and encapsulation efficiency of $97.2 \pm 3.9\%$. TEM study showed the spherical shape particles. The in-vitro drug release revealed $62.1 \pm 0.5\%$ release of CAB in simulated gastric buffer (pH 1.2) and $45.5 \pm 2.8\%$ in physiological buffer (pH 7.4). In-vitro cytotoxicity study and antibacterial activity depicted the safety of the prepared NPs by showing lesser toxicity than pure CAB. From the results, our experimental outcomes concluded that CAB gold nanoparticles composed of pectin may constitute a preferred embodiment for the delivery of CAB.

Keywords Cabotegravir · Gold nanoparticles · Cytotoxicity · Box–Behnken · Antibacterial · Biopolymer

Introduction

The human immunodeficiency virus (HIV) is one of the world's deadliest pandemics until now [1]. As per the findings of UNAIDS [2, 3], about 30.2 to 45.1 million people worldwide suffered from HIV/AIDS in 2020, of which 1.2 to 2.2 million were children (< 15 years old) and 38.9 to 43.2 million were adults (53% females). WHO (after consideration of the effect of the COVID 19 pandemic) also reported that more than 0.68 million individuals died from HIV related causes in 2020 and around 1.5 million are newly affected [1].

HIV contains RNA as a viral-coated genetic material and is a member of the retrovirus family. Initially, the virus enters the host cell and removes its cover to fabricate another different kind of genetic material (provirus). It gets incorporated into DNA and captures the host cell apparatus to start creating so many countless new virion particles. Hence, the HIV life cycle becomes dreaded to find an appropriate treatment [4–7]. Nowadays, there are seven categories of anti-HIV drugs that are used to target different stages of the HIV life cycle [8, 9]. Most of the anti-HIV drugs have been reported for poor bioavailability due to the low solubility or first-pass effect. The overall influence is depending upon the repercussion due to the development of drug resistance or other adverse effects arising owing to the discontinuation of therapy. The virus can reproduce in the systemic circulation and continue to propagate the infection [10, 11].

Cabotegravir (CAB) is an HIV-1 specific integrase strand transfer inhibitor (INSTI), from the carbamoyl pyridone class. It is an analogue of dolutegravir that prevents viral DNA integration into the host genome and inhibits HIV replication. It is highly lipophilic and falls under the BCS class II drug. The long systemic half-life (~ 40 h) makes long-acting CAB injectable formulation a

✉ Purnima Rawat
purrnimanegi@gmail.com

1 Discipline of Biosciences and Biomedical Engineering, Indian Institute of Technology, Madhya Pradesh, Indore 453552, India

2 Department of Pharmaceutics, College of Pharmacy, King Saud University, Riyadh 11451, Saudi Arabia

potential candidate for the treatment and prevention of HIV [12–14]. Cabotegravir has a major drawback of poor absorption in the gastric fluid that leads to a significant reduction in its bioavailability [14–17]. The concept of nanoparticulate delivery can overcome numerous side effects like diarrhea, headache, pyrexia, fatigue, sleep disorders, nausea, dizziness, flatulence, and abdominal pain [18]. Another study revealed that inflammatory tissue response associated with cabotegravir long-acting injection can play a key role in the breakdown, absorption, and systemic dissemination of CAB from injection sites [19].

In the recent past, researchers have already established that metallic nanoparticles such as gold, silver, titanium oxide and iron may breathe new life into the field of delivery systems [20–21]. Among these, gold NPs is widely used due to their non-toxic and inert nature [22–24]. For biological applications, gold NPs coated with PEG or in combination with other molecules such as biotin, peptides, or oligonucleotides have been synthesized [25–27]. The ability of gold NPs to inhibit VPF/VEGF induced endothelial cell proliferation provides compelling evidence of their therapeutic potential in different diseases [28–29]. Thus, the use of gold NPs could play a crucial role in diseases like cancer and HIV by providing a significant target with nano vehicles [30]. Since the properties of nanoparticles depend on the size, one of the major limitations in the in-vivo application of NPs is the effect of aging. Any physical instability in the NPs with time (or due to biological medium) will limit their pharmaceutical applications in the real world [31]. Several studies in the past have been focused on the effect of aging in the stability of nanoparticles [32–38]. Researcher have used numerous types of biopolymers such as gellan gum [39], xanthan gum [40], chitosan [41] and pectin [42] to avoid Agglomeration, precipitation and even chemical or physical decomposition of nanoparticles. Pectin, a naturally occurring polysaccharide, offers a most suitable green route for stabilization due to its high biocompatibility, biodegradability, cost effectiveness and non-toxic nature [43–46]. Rationalized by earlier studies, we incorporated pectin in the structure of nanoparticles to further enhance GNPs stabilities.

In the management of HIV/AIDS, the route of administration (intramuscular, intravenous, intradermal, oral etc.) play a critical role in achieving drug efficacy. In the treatment of HIV, parenteral delivery is a commonly used route of administration [47–48]. The application of parenteral formulations has limitations of vasovagal or presyncopal reactions, lesions and irritation [49–50]. Thus, a better drug delivery system is needed to ensure the controlled drug release, supporting the effective concentrations over a long time, thus providing uninterrupted treatment.

In the present study, we prepared Cabotegravir gold nanoparticles (CAB-GNPs), followed by their optimization using Box–Behnken Design (BBD) to obtain the optimum formulation composition (i.e., minimum size and maximum encapsulation efficiency). The formulations were optimized using independent variables as gold chloride (A), pectin (B) and pH (C) to get the appropriate particle size (PS as Y^1) and encapsulation efficiency (EE as Y^2). The selected nanoparticles were further evaluated for percentage yield, drug release, x-ray diffraction, in-vitro cytotoxicity, and antimicrobial assessment. The antimicrobial activity was also evaluated because under a weaker immune system, the individual becomes extremely prone to various kinds of viral or bacterial infections, which may lead to death [51–53]. There are different bacteria that may lead to infection to the weaker immune patients. The use of antibacterial agent can result the emergence of antibiotic-resistant bacteria and complicate the treatment of HIV infection. In the light of these factors, we have taken CAB-GNPs as gold nanoparticles have excellent antibacterial property [54–55]. It was reported that in early trials of healthy and HIV-1 infected people, oral CAB doses were generally well tolerated [17]. When taken as prescribed, it is highly effective at reducing HIV acquisition risk [56–57]. Poor bioavailability of oral route administration may also be enhanced with the use of nanoparticles-loaded drug [58–60]. According to a recent CDC report, modern oral antiretroviral therapy could prevent HIV viremia even with single tablet dosing per day [61]. Although a lot of research is going on single/combination therapy of HIV drugs through the oral routes, it is still not enough to reach their full potential in reducing new HIV infections [58–61].

Materials and Methods

Materials

Cabotegravir (CAB) was purchased from Invivo chem (Libertyville, USA). Tetrachloroauric acid trihydrate (Sigma-Aldrich, USA), pectin (Loba Chemie, India), tween 60 (Sigma -Aldrich, USA) were used as received without additional purification. Milli Q water and AR grade chemicals were used for the experiment.

Methods

Fabrication of Gold Nanoparticles

The slightly modified reported method by Turkevich et al. was used to synthesize CAB gold NPs. [22, 23, 62, 63]. The colloidal dispersion of $AuCl_4$ was prepared by the reduction of tetrachloroauric acid

(gold chloride). Different concentration of gold chloride (1 to 3 mM) was added to pectin solution in a concentration of 0.01 to 1% (w/v) for 10–15 min at a basic pH range of 11–13. The prepared dispersion was converted to ruby red from blue colour. The synthesised gold NPs were dialyzed for 12 h with double distilled water in which the dispersion of the pH was found to be 7. A calculated amount of drug (CAB) was dispersed in tween 60 solution (0.1 nmol/L) and then added to a gold NPs dispersion with a resultant CAB concentration of 5 mM in 100 mL solution. The concentration of each variable used to prepare gold NPs are mentioned in Table 1. The mixture was incubated for 24 h at room temperature and then centrifuged at 30,000 rpm for 2 h to remove excess drug. The collected pellet was separated from the supernatant solution and re-dispersed in water for further characterization.

Design of Experiment

In the present study, Box–Behnken design (Design Expert® 12, Statease) has been employed to optimize the gold NPs (GNPs). The optimization was performed using 3 factors: gold chloride (A), pectin (B), and solution pH (C) at 3 levels (low, medium, high). The effect of independent variables was evaluated on the dependent variables as PS (Y^1) and EE (Y^2). The design showed 15 formulation runs with 3 common compositions to check the error during the preparation. The different models like linear, quadratic and 2F were used to evaluate the optimization process. The ideal model for the selection of optimized

formulation is the quadratic model in which the selected independent variables showed the individual as well as combined effects. The p-value of the regression coefficient was also used to evaluate the significant factors over the responses. Further, ANOVA was also applied to determine the significance of the model. The software generated polynomial equation of each factor was used to evaluate the negative and positive effects on the PS and EE [64]. The predicted and actual value of each response was used to validate the method. Finally, the selected optimized NPs were characterized for physicochemical properties.

Evaluation Parameters

Particle Size (PS), Polydispersity Index (PDI) and Surface Charge (ZP)

The prepared CAB-GNPs were evaluated for PS, PDI and ZP using a particle size analyzer (Malvern Zetasizer, Malvern, UK). PDI is used to measure the particle size distribution and the value below 0.7 is considered uniform [21, 23]. GLN-7 (0.1 ml) was dispersed in double distilled water and transferred to a cuvette for the analysis. The same sample was taken in the cuvette with an electrode to measure the ZP.

Encapsulation Efficiency (%EE)

The experiment was carried out to evaluate the amount of CAB encapsulated in the prepared nanoparticles by the

Table 1 Box Behnken design based experimental runs and their responses used for the formulation of CAB gold nanoparticles

1. Formulation	Independent variables			Responses (mean ± SD; n = 3)	
	Gold chloride (mM); X^1	Pectin (%); X^2	pH; X^3	Size (nm); Y^1	Entrapment efficiency (%); Y^2
GLN-1	1	1.00	12	17.1 ± 0.1	82.7 ± 1.4
GLN-2	3	0.51	11	65.3 ± 0.3	57.4 ± 2.9
GLN-3	2	0.51	12	34.5 ± 0.2	72.5 ± 1.3
GLN-4	3	1.00	12	86.8 ± 0.3	65.9 ± 2.5
GLN-5	2	0.01	13	31.7 ± 0.2	79.5 ± 3.1
GLN-6	3	0.51	13	78.1 ± 0.2	68.7 ± 2.4
GLN-7	1	0.01	12	3.1 ± 0.2	94.1 ± 1.3
GLN-8	1	0.51	11	7.5 ± 0.2	89.8 ± 1.7
GLN-9	2	0.51	12	34.1 ± 0.3	71.9 ± 2.1
GLN-10	2	0.51	12	35.9 ± 0.2	71.1 ± 1.9
GLN-11	2	0.01	11	25.8 ± 0.1	77.8 ± 1.7
GLN-12	2	0.51	13	9.4 ± 0.2	86.2 ± 2.9
GLN-13	2	1.00	13	51.9 ± 0.1	73.7 ± 3.2
GLN-14	2	1.00	11	44.8 ± 0.3	67.4 ± 3.2
GLN-15	3	0.01	12	65.2 ± 0.2	63.1 ± 1.7

indirect method. The sample of GLN-7 (2 mL) was taken and centrifuged for one hour at 10,000 rpm. The supernatant of the centrifuged dispersion was taken, diluted, and assayed spectrophotometrically (Perkin Elmer, LAMDA-35) at 537 nm. Each formulation was evaluated three times and the mean encapsulation efficiency was evaluated using the formula:

$$\%\text{Encapsulation efficiency}$$
$$= \frac{\text{Weight of initial CAB} - \text{Weight of free CAB}}{\text{Weight of initial CAB}} \times 100$$

Percentage Yield

The prepared CAB-GNPs (GLN-7) were collected and weighed accurately to evaluate the percentage yield. The individual weight of each ingredient was also taken to calculate the percentage yield of the nanoparticles using the following Eq. (28).

$$\%Yield = \frac{Tm}{Ti} \times 100$$

Tm total weight of dried nanoparticles; Ti total dry weight of all added components.

Transmission Electron Microscopy (TEM)

The surface morphology of the prepared CAB-GNPs (GLN-7) was studied using TEM (TECHNAI- Fei, Electron optics, USA). CAB-GNPs (GLN-7) dispersion was applied in the form of a droplet to the carbon-coated grids and dried at room temperature. The image of the NPs was taken at a 200 kV accelerated voltage [25].

XRD Analysis

XRD analysis was done to evaluate the crystalline structure of CAB and CAB-GNPs (GLN-7) using a diffractometer (Rigaku X-ray diffractometer, Japan). The sample was measured at an applied current of 30 mA, accelerating voltage 40 kV in a 2θ angle configuration with CuKα radiation (λ = 1.54 Å). The sample was scanned with a scanning rate of 2°/min, in the measurement range of 20° to 80° [25, 75].

Drug Release

The drug release study was done to determine the CAB release from the optimized CAB-GNPs (GLN-7) on two different media. The drug release was carried out in phosphate buffer saline (pH 7.4) and simulated gastric buffer (pH 1.2) with 2% tween 80 using the dialysis bag for

24 h [48]. The pre-soaked dialysis bags (MWCO 12–14 kD, Himedia) was taken to study the release profile. The samples GLN 7 as well as pure CAB dispersion (~ 0.5 mM CAB), were filled into the dialysis bag. The samples containing bag is dipped into the dissolution media (250 mL with 2% tween 80). The tween 80 was added into the release media to maintain the sink condition of CAB. The temperature was fixed at 37 °C with a stirring speed of 100 rpm. The released content (5 mL) was collected at a specific time and replaced with the same volume. The sample was diluted further to determine CAB content at several time points using UV-spectrophotometer at 537 nm. All the procedures were carried out three times. The released data were fitted into different mathematical models to determine the release mechanism [66–68].

Antibacterial Activity

The minimum inhibitory concentration of CAB-GNPs (GLN7) was evaluated in LB (Lysogeny broth) medium against the gram-positive organism (S. aureus) and gram-negative organism (E. coli). CAB-GNPs of different concentrations (0, 1, 5, 10, 20 μg/mL) were added to the medium with a bacteria cultures load of 10^5–10^6 CFU/mL and then incubated at 35 °C. The optical density of each sample was measured after 24 h to evaluate the minimum inhibitory concentration (MIC) [68]. Further, the sample was evaluated for antibacterial activities of S. aureus and E. coli bacteria using the agar well diffusion process [69]. Before being tested, the bacteria were kept in broth and sub-cultured in a petridish. The test sample CAB-GNPs were added to sterile Mueller Hinton plates well. The positive control gentamycin (0.1 mg/mL) was taken to compare the result. The plates were incubated for 24 and 48 h in an incubator and inhibition zones diameter (mm) was determined in triplicate.

Cytotoxicity Study

The cellular effect of CAB-GNPs on enzymatic behaviour was measured using the MTT assay. The reagent (3-[4, 5-dimethylthiozol-2-yl]-2,5- diphenyl tetrazolium bromide) was metabolized by viable cells after exposure to NPs. The colour of cell culture turns purple after forming an insoluble formazan crystal. Cancer cells (HeLa) and Human embryonic kidney cells (HEK 293), cultured and maintained in DMEM media (supplemented with 10% Fetal Bovine Serum (FBS)) were incubated in an incubator at 37 °C with a CO_2 flow. The cells were trypsinized with trypsin–EDTA solution (0.25% trypsin, 1 mM EDTA) and seeded at a density of 1×10^4 cells per well in 96 well plates. The plates were kept in a CO_2 incubator at 37 °C for 24 h. CAB-GNPs were added to each well and incubated

for 3 to 4 h in fresh media containing MTT reagent (10 µL). 200 µL of DMSO was incorporated into each well to dissolve the formazan crystals formed in the viable cells. The solution's absorbance was measured at 540 nm using (Bio Tek Synergy H1) microplate reader. The untreated cells with NPs were considered as control, and the relative viability of the cells was measured [68].

Stability Study

The stability study of the prepared CAB-GNPs (GLN-7) was performed to evaluate the changes after storage at 30 °C ± 2 °C/65% RH ± 5% RH [61]. The sample was stored in glass vial and analysed for particle size and encapsulation efficiency at specific time intervals (0, 3 and 6 months) [70].

Results and Discussion

Optimization

CAB-GNPs were prepared and further optimized using Box Behnken design. The variables used to optimize gold chloride (A), pectin (B) and pH (C) are shown in Table 1. These variables were taken at three-level (low, medium, high) and the formulation composition effects were assessed on PS (Y^1) and EE (Y^2) (Fig. 1A, B). For every formulations; size, PDI, zeta potential and encapsulation efficiency were evaluated. The factors which got significantly affected by the variation of the independent variables were selected for the optimization process. It was found that the result of PDI and ZP have no significant effect. The design showed 15 different compositions with three common formulae to check the error. The optimization was performed using different mathematical models (linear, 2 F1, quadratic and cubic) given by the software. The quadratic model is considered an ideal model because it shows the individual as well as a combined effect of the used variable on the PS and EE. The results revealed the highest values for both adjusted and predicted regression coefficients and considered as a best-fit model (> 0.9).

Effect on Particle Size (Y^1)

The independent factors gold chloride (A), pectin (B), and pH (C) showed a marked effect on the PS (Y^1). A significant difference in the size was observed. The minimum PS was found to be 3.1 nm for formulation (F7) having the following composition: gold chloride (1 mM), pectin (0.01%) and pH-12. The maximum PS was observed for the formulation (GLN-4) having the composition: gold chloride (3 mM), pectin (1%) and pH-12. The variation in the PS was observed due to the variation in the composition
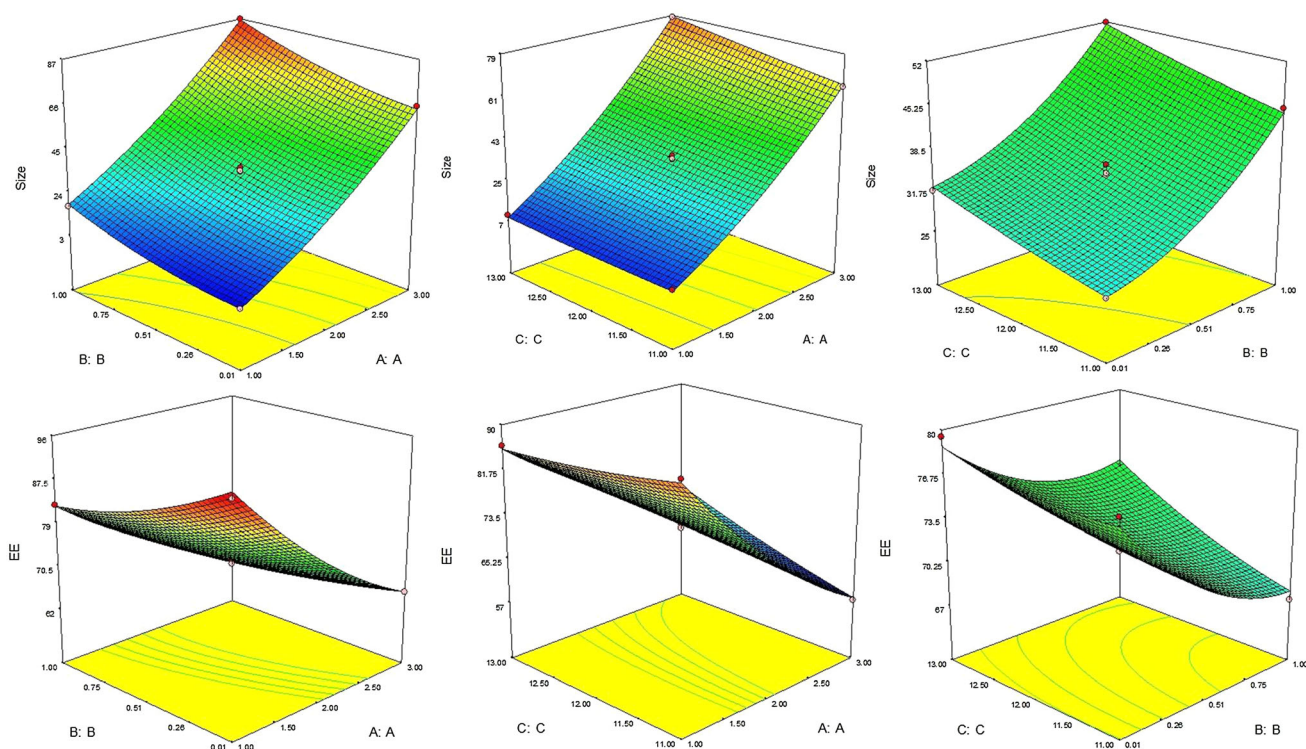
Fig. 1 3D contour plot showing the effect of independent variables on dependent variables particle size (Y^1) and encapsulation efficiency (Y^2)

of independent variables. The effect of independent variables on the PS could be well observed from the polynomial equation and 3D response surface plot (Fig. 1a). The quadratic equation governing the PS of the gold NPs is as follows:

$$\begin{aligned} \text{Particle Size} = & +34.83 + 32.29A + 9.35B + 3.46C \\ & + 1.9AB + 2.72AC + 0.3BC + 4.87A^2 \\ & + 3.35B^2 + 0.37C \end{aligned}$$

The polynomial equation shows that the independent variables have individual as well as combined effects on the PS. ANOVA of individual terms of the PS equation revealed that the factors A, B, C, AB, AC, BC, A2, B2, and C2 are found to be significant model terms. Additionally, both hydrophilic polymers (gold chloride and pectin; factors A and C) showed a positive impact on the PS. A rise in gold chloride concentration (A) resulted in a larger globule size in the primary suspension. An increase in pectin concentration (B), also depicted an increase in PS. At higher concentration, the pectin adsorption increases on the particle surface of the primary suspension, and thus a larger size of gold NPs. Furthermore, during the formation of the primary suspension, the pH range (C) had a major negative impact on the size, i.e., an increase in pH range resulted in a decrease in PS of the primary suspension, which in turn directed the formation of smaller size NPs. The findings were also significantly influenced by the other combined interaction terms (AB, BC, and AC). A change in one-factor magnitude will almost certainly affect the response generated by changes in other factors. All statistically relevant higher-order terms (A2, B2, and C2) has a nonlinear relationship with the PS of the NPs.

Effect on Encapsulation Efficiency (Y^2)

The independent factors gold chloride (A), pectin (B) and pH (C) showed a significant effect on the EE. The minimum EE of 57.4% is shown by the formulation (GLN-2) having the composition: gold chloride (2 mM), pectin (0.5%) and pH-12. The maximum encapsulation efficiency of 94.1% was observed for the formulation (GLN-7) having the composition: gold chloride (1 mM), pectin (0.01%) and pH-12. The variation in the EE was observed due to the variation in the composition of independent variables. The effect of independent variables on the EE could be well observed by the polynomial equation and 3D response surface plot (Fig. 1B). The quadratic equation governing the encapsulation efficiency of the gold NPs is as follows:

$$\begin{aligned} \%EE = & +71.83 - 1.92A - 3.39B + 1.97C + 2.97AB \\ & + 3.74AC + 1.15BC + 3.07A^2 + 2.13B^2 \\ & + 0.64C^2 \end{aligned}$$

A, B, C, AC, AC, A^2, B^2, C^2 are all significant model terms ($p < 0.05$) as shown by the polynomial equation and ANOVA results. The concentration of gold chloride (A) and pectin concentration (B) have shown a negative influence on EE. With the increase in gold chloride concentration (A) and pectin concentration (B), the EE was decreased. It may be due to the highly lipophilic character of the drug (CAB). The variable (A) has shown a greater effect than variable B. But the third variable 'pH' (C) showed a positive effect on EE. A higher pH might have led to enhanced encapsulation from the hydrophilic gold coating. The other combined interaction terms (AB, BC, and AC) were also found to have a significant positive effect on the results. The combined factors (gold chloride and pectin, AB) have shown a positive effect on encapsulation efficiency. The combination of these factors helps to get greater encapsulation of CAB in the specific ratio. A similar effect is obtained by the blend of gold chloride (A) and pH of the solution (C) as well as pectin (B) and pH (C). The factors AC and BC have shown greater effect than the factor AB. A change in one-factor magnitude will almost certainly influence the response produced by other factors. All statistically significant higher-order terms (A^2, B^2, and C^2) was found to have a nonlinear relationship with encapsulation efficiency. The polynomial equation interpretation is well supported with the 3D-response surface graph (between encapsulation efficiency and various factors).

Point Prediction

To get the minimum PS and maximum EE, the software used the point prediction method to select optimized composition. Out of 15 formulas given by the software, the formulation (GLN-7) having the composition: gold chloride 1 mM (A), pectin 0.1% (B) and pH 12 (C) showed the PS of 3.1 nm with an EE of 94.1%. The optimized formulation (GLN-7) prepared with the composition: gold chloride 1 mM (A), pectin 0.1% (B) and pH 12 (C), showed the PS of 3.9 ± 0.1 nm with an EE of $97.2 \pm 3.9\%$. The software generated predicted PS and EE were found to be 3.8 nm and 95.6% respectively. The close results of actual and predicted values confirm that the user process is accurate. The predicted and actual attribute of the optimized formulation is shown in Table 2. The overall desirability for each factor was found to be closer to unity (0.95 and 0.98) for size and encapsulation efficiency. The statistical analysis was also found well in agreement with the point prediction value of each factor. The statistical analysis of the size and encapsulation efficiency is presented in Table 3. Among the four statistical parameters, the best-fit model was found to be for the quadratic model.

Table 2 Predicted and actual values of the optimized CAB gold nanoparticles (GLN-7)

Formulation	Composition			Characterization	
	Gold chloride (X^1)	Pectin (X^2)	pH (X^3)	Particle size (nm)	Encapsulation efficiency (%)
GLN-7 (predicted)	1.1 mM	0.2%	12.5	3.8	95.6%
GLN-7 (actual)	1 mM	0.1%	12	3.9 ± 0.2	97.2 ± 3.9
% Error	–	–	–	0.27	1.67

Table 3 Statistical analysis of different model used to optimize CAB gold nanoparticles

Model	Size (Y^1)			Entrapment efficiency (Y^2)		
	R^2	Adjusted R^2	Predicted R^2	R^2	Adjusted R^2	Predicted R^2
Linear	0.9815	0.9764	0.9673	0.8924	0.8631	0.7908
2F1	0.9863	0.9760	0.9559	0.9609	0.9316	0.8809
Quadratic	0.9992	0.9978	0.9901	0.9951	0.9864	0.9318

Characterization

Particle Size (PS), Polydispersity Index (PDI) and Surface Charge (ZP)

The mean particle size range of the CAB gold NPs was found in the range of 3.1 nm (GLN-7) to 65.3 nm (GLN-2). The optimized CAB gold NPs showed the PS of 3.9 ± 0.1 nm and surface charge of -33.1 ± 0.5 mV (Fig. 2A, B). The significant variations in the PS are due to the change in the composition of independent variables. The optimized CAB gold NPs showed a low polydispersity index (PDI) value of 0.5 ± 0.1, indicating the uniform particle size distribution which is ideal for the greater drug release due to the smaller particle size distribution.

Encapsulation Efficiency

GLN-7 showed encapsulation efficiency of 97.2 ± 3.9%, indicating that the experimental process and structure are suitable for the encapsulation of a high concentration lipophilic drug in the hydrophilic gold chloride ($AuCl_4$) (Table 4). One of the primary targets for improving encapsulation efficiency is the outer layer of hydrophilic pectin that protects the CAB from oozing out [67, 69].

Percentage Yield

The optimised formulation GLN-7 percentage yield was found to be 92.5 ± 2.4%, indicating the low process loss. The increase in pectin concentration will influence it, and hence a improved practical yield.

Transmission Electron Microscopy (TEM)

TEM analysis revealed that the CAB gold NPs (GLN-7) are spherical in shape with no aggregation (Fig. 2C, D). This is due to the capping of pectin which stabilized the individual NPs.

X-Ray Diffraction

The powder XRD diffractogram of CAB (drug), gold nanoparticles (GNPs) and CAB gold NPs (GLN-7) are depicted in Fig. 3. The presence of intense diffraction peaks indicates the formation of crystalline gold (Au). The presence of AuNPs peaks were reflected radiation (Bragg peaks) at 31.3°, 45.3°, 65.9° and 74.9° corresponding to characteristic diffractions of (111), (200), (220) and (311) planes. CAB showed the peaks at 6.8°, 15.9°, 18.5°, 20.8°, 23.9°, 26.4°, and 28.9° and CAB gold NPs (GLN-7) showed the peaks at 6.8°, 28.4°, 34.3°, 43.6°, 65.3°, and 74.9°, respectively. The mean average size of crystals was calculated using the Debye–Scherrer Eq. (71). The line width of (111) plane was considered for the calculation. The Debye–Scherrer equation is given as follows:

$$d = \frac{k\lambda}{\beta \cos \theta},$$

where, 'd' is the mean size of the crystalline domains, 'k' is dimensionless shape factor, with a value close to unity (0.9), 'λ' is a wavelength of X-ray, 'β is the width at half-maximum of the (111) peak in radians, 'θ' is the angle of diffraction. The size of crystal of CAB gold NPs (GLN-7)
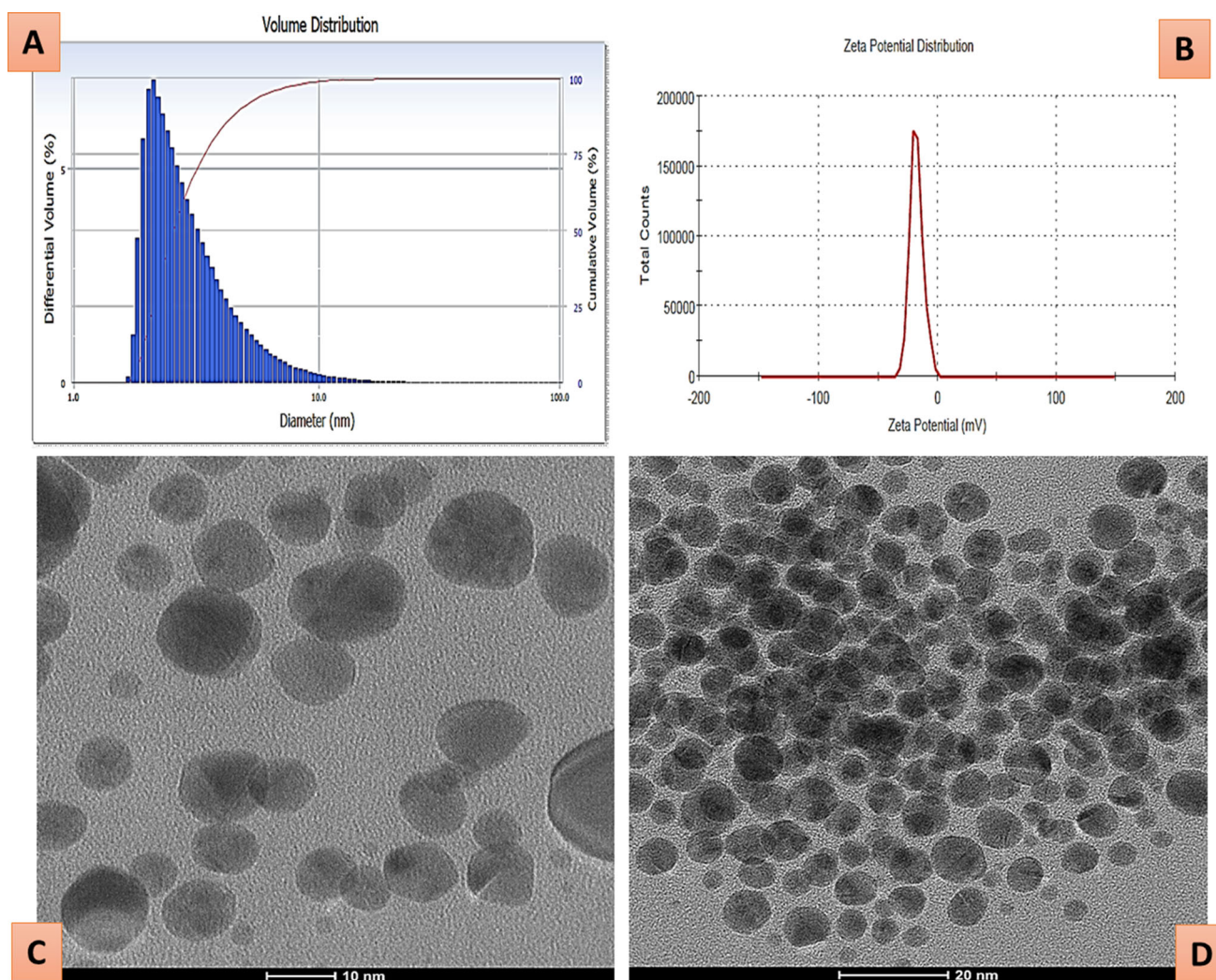
Fig. 2 A CAB gold nanoparticle particle size distribution, B zeta potential, C HRTEM and (D) TEM images

Table 4 In vitro release model fitting for CAB gold NPs (GLN-7) in different release media

| Model | Stimulated Gastric buffer (pH 1.2) | | | | Phosphate buffer saline (pH 7.4) | | | |
| | CAB suspension | | CAB-GNPs (GLN-7) | | CAB suspension | | CAB-GNPs (GLN-7) | |
	R	K	R	K	R	K	R	K
Zero-order model	0.9516	27.9748	0.3057	3.7540	0.8416	14.1019	0.6374	2.4377
First-order model	0.9364	− 0.9119	0.6618	− 0.0554	0.9887	− 0.4372	0.7433	− 0.0305
Higuchi model	0.9953	49.0012	0.9308	15.7106	0.9743	35.3278	0.9527	9.9627
Hixson–Crowell model	0.9926	43.5189	0.5775	− 0.0161	0.9847	− 0.0901	0.7115	− 0.0094
Korsmeyer–Peppas model	0.9946	43.5189	0.9400	15.8792	0.9645	27.2835	0.9121	6.0418

determined by the given equation was found to be in the range of 3–14.0 nm. The estimation of size using the equation was in confirmation with diameter of synthesized gold NPs (AuNPs) obtained from TEM [72].

Drug Release

Figure 4 shows the comparison of CAB release from CAB suspension and CAB gold nanoparticles (GLN-7) in phosphate buffer saline (pH 7.4) and simulated gastric

buffer (pH 1.2). CAB release from the CAB suspension at pH 1.2 was observed to be 99.9 ± 0.4 within 4 h of study. However, CAB release from gold NPs (GLN-7) showed $62.1 \pm 0.5\%$ release in 24 h. In the phosphate buffer saline (pH 7.4), the release from CAB suspension is found to be
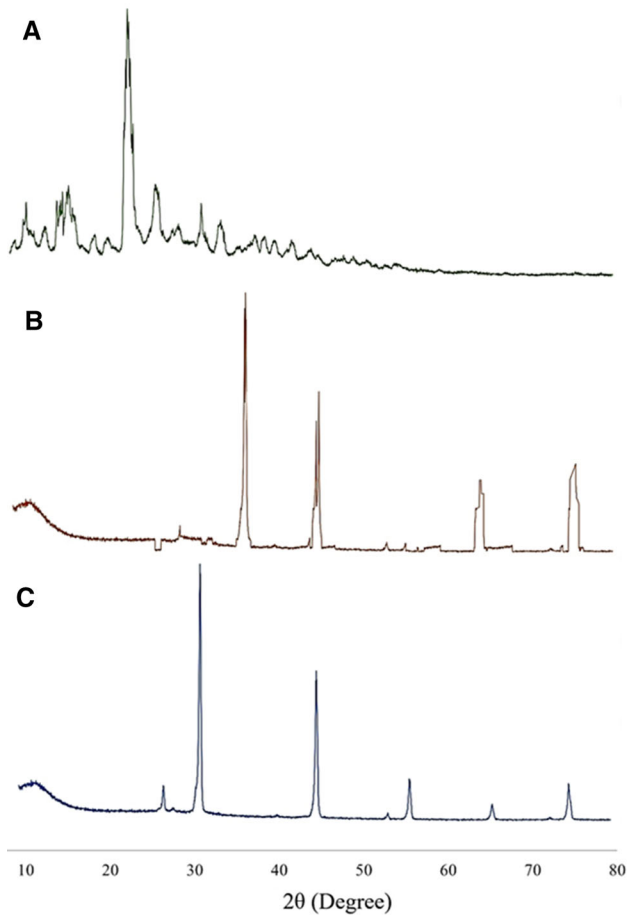
Fig. 3 XRD patterns of **A** cabotegravir, **B** blank gold nanoparticles and **C** CAB load gold nanoparticles (GLN-7)
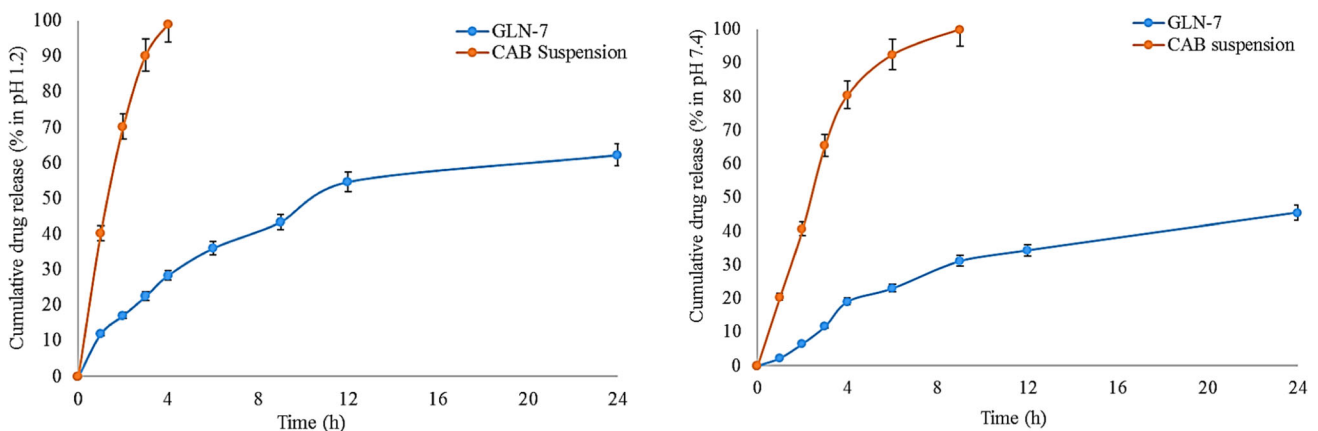
$99.9 \pm 1.6\%$ in 9 h, whereas CAB gold nanoparticles (GLN-7) depicted only $45.5 \pm 2.8\%$ release. The relative release profile of both media demonstrated that the drug dissolution behaviour is affected by pH. The drug release mechanism was calculated, and the best model was chosen based on the highest values of regression coefficients (actual and adjusted), as seen in Table 4. The best-fitting model in both the media was found to be the Higuchi model in pH 7.4 media and the Korsmeyer–Peppas model in pH 1.2 media. The Higuchi drug release model is a typical release pattern through a polymeric matrix in which the shape of the system remains constant and release occurs via diffusion. [67]. Korsmeyer-Peppas model, also known as the power law, is a semi-empirical relation in which the fraction of drug release is exponentially proportional to the time it takes for the drug to be released and the release must take place in a single dimension. By releasing the drug radially outward from the source, the single dimension is formed, allowing a one-dimensional problem to be modelled [66, 67]. Since, CAB has a long $t_{1/2}$ of 40 h, the continuous release of GLN-7 would be beneficial. As a result, this mechanism is capable to control the drug release and is independent of any interference with the medium [66, 68].

Antibacterial Activity

MIC level of the CAB gold nanoparticles (GLN-7) was evaluated against *E. coli* (Gram-negative bacteria) and *S. aureus* (Gram-positive bacteria). The different concentration was evaluated to select the one concentration and further assessed for antibacterial activity. The inhibition kinetics of the different concentrations of CAB gold NPs were evaluated in *E. coli* and *S. aureus* as shown in Fig. 5. MIC of the CAB-gold NPs was found to be 10 µg/mL for both *S. aureus* and *E. coli*. At high

Fig. 4 In-vitro release of CAB suspension and CAB gold nanoparticle (GLN-7) at two different pH (1.2 and 7.4). Each study performed in triplicate and data shown as mean $\pm$ SD
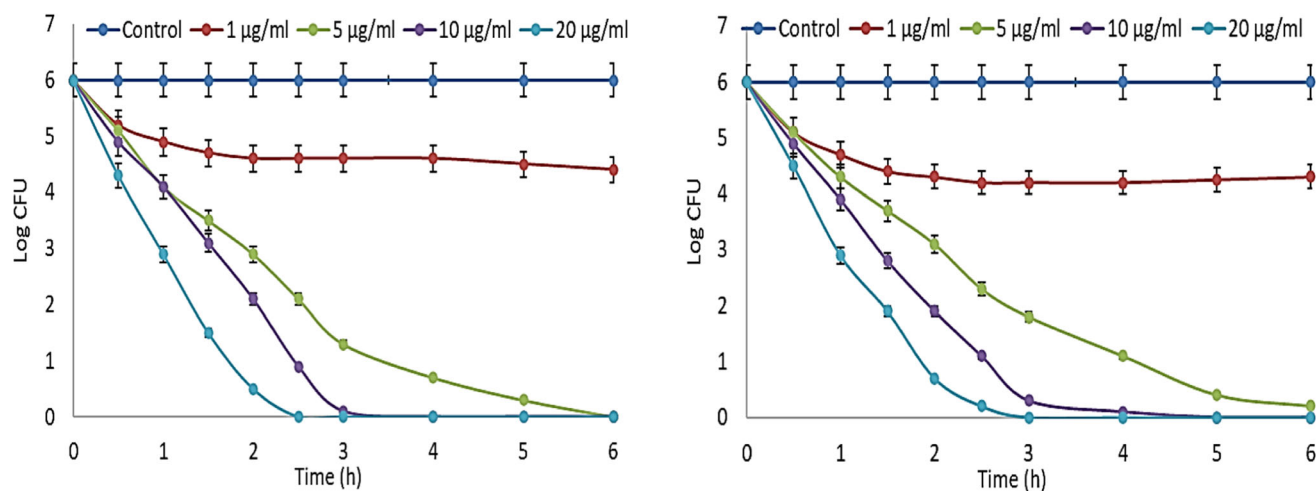
Fig. 5 Growth inhibition effect of the CAB gold nanoparticles on *E. coli* and *S. aureus* at
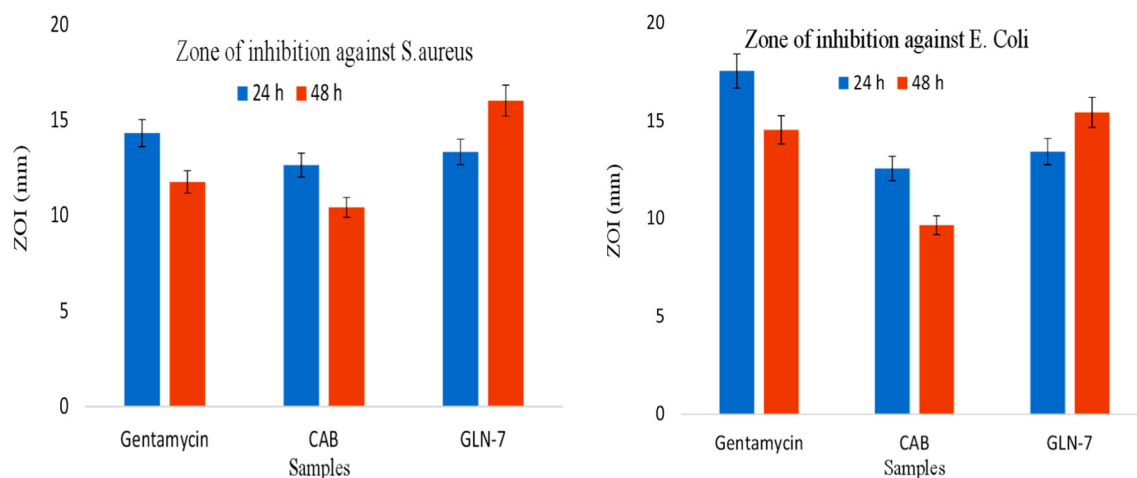
Fig. 6 Zone of inhibition (mm) of *S. aureus* and *E. coli* for the CAB gold nanoparticles (GLN-7). Each study performed in triplicate and data shown as mean ± SD

concentration, the viable cells were inhibited within 2.5 and 3 h for *E. coli* and against *S. aureus*, it showed the inhibition within 2 and 3 h. 5 ppm concentration was not enough to inhibit both organisms within tested time. The gold nanoparticles showed a lower MIC value over GLN-7, due to the smaller size of the nanoparticles and the negative surface charge of pectin interferes with microbial absorption on the surface of gold nanoparticles. It was reported in S.M. Navarro Gallon., et al. that the narrow size of nanoparticles influenced the antibacterial activity due to the specific surface area for interaction with the bacterial membrane [73]. The antibacterial activity of CAB gold nanoparticles (GLN-7) was evaluated against *E. coli* and *S. aureus*, in a fixed-dose for different time points and result shown in Fig. 6. The growth of the bacteria is treated, as well as untreated well with gold nanoparticles was investigated. The standard gentamycin

showed the ZOI of 14.3 ± 1.8 mm at 24 h and 11.7 ± 0.8 mm at 48 h. The antibacterial effect was found to be higher at 24 h than 48 h. In the case of pure CAB, a similar type of effect was found with standard gentamycin. The sample showed a higher effect at 24 h (12.6 ± 1.3 mm) than 48 h (10.9 ± 0.7 mm). CAB gold NPs showed a higher effect at 48 h (14.0 ± 0.8 mm) than 24 h (16.3 ± 1.3 mm). The greater effect may be due to the slower release of CAB from gold NPs as well as gold also reported for the antibacterial property. The presence of gold chloride and CAB showed synergistic effect on the tested organisms. The gold NPs adsorb on the surface of bacteria and inhibit the intracellular enzymatic activity [69, 74–75]. The zone of inhibition was also evaluated against *E. Coli* and the result showed a similar type of effect (Fig. 5). The zone of inhibition against *E. coli* after treatment with standard gentamycin, pure CAB and CAB-

NPs (GLN-7) were found to be 17.1 ± 2.6 mm, 12.5 ± 1.3 mm, and 14.4 ± 2.3 mm, respectively at 24 h. The same concentration was also evaluated for 48 h and the result depicted significant ($p < 0.05$) changes in the results. The standard gentamycin showed a smaller zone of inhibition with 14.1 ± 1.3 mm, pure CAB also revealed lesser effect (9.6 ± 0.8 mm) than 24 h treated well. In the case of CAB gold nanoparticles (GLN-7), the enhanced effect was observed at both time points than pure CAB. At 24 h, the ZOI was found to be 14.4 ± 2.3 mm and at 48 h, the ZOI was found to be 15.9 ± 1.6 mm. CAB gold nanoparticles (GLN-7) showed prolonged effect due to the slower CAB release from the gold NPs. The other reason for the enhanced effect is the antibacterial activity of the gold which gives synergistic action to the drug CAB.

In-Vitro Cytotoxicity

An MTT assay was used to assess the *in-vitro* cytotoxicity of CAB gold nanoparticles (GLN-7) and was shown in Fig. 7. GLN-7 was incubated with immortal HeLa cells and HEK-293 for 24 h with different concentrations. The viability of the cells was compared to healthy cells that had not been incubated with any sample groups (control). The cell viability of the GLN-7 treated group showed sustained effect up to 90% after incubation at a concentration of 5 µg/mL. In addition, MTT results also showed that GLN-7 had less than 10–20% cytotoxicity in both HeLa and HEK-293 cells at a higher concentration of CAB gold nanoparticles. The earlier reported data suggested that the HEK-293 (immune) and HeLa (non-immune) cells didn't induce significant cytotoxicity up to 28 days in ritonavir, lopinavir, and efavirenz loaded nanoparticles [76]. HeLa and HEK-293 are widely used as these cells are transduced to the cell surface expression of receptor CXCR4, CCR5 and

CD4 which are susceptible to HIV infection [77]. It was observed that as the concentration of gold nanoparticles increases the cytotoxicity increases as well. When compared to the control group with CAB gold nanoparticles demonstrated higher cell viability [78–79]. As a result, the encapsulation of the drug has little impact on the in-vitro cytotoxicity of gold nanoparticles. The CAB gold nanoparticles (GLN-7) were found to be non-toxic and suitable for in-vivo applications [68, 76].

Stability Study

There were significant changes observed in the particle size and encapsulation efficiency. The initial (0 month) particle size was found to be 3.9 ± 0.1 nm. A non-significant change in the size was observed after 3 months (particle size after three months: 4.1 ± 0.3 nm). A considerable increase in the particle size was observed at 6 months (9.2 ± 0.8 nm) from 3 months, the difference was found to be significant. A significant ($p < 0.05$) difference was found at 6 months from initial particle size. PS was found to be slightly higher after six months. The particle size evaluation showed a stable formulation for prolonged period. The better stability was due to the optimum ZP and PDI value. The selected formulation (GLN-7) was also evaluated for encapsulation efficiency (EE). The result showed slight changes in the encapsulation efficiency. The initial encapsulation efficiency was found to be $97.2 \pm 3.9\%$. The sample was stored for 3 months and 6 months to evaluate encapsulation efficiency. After 3 months the encapsulation efficiency was decreased and found to be $95.1 \pm 4.2\%$. The difference was found to be non-significant. The encapsulation efficiency further decreased after 6-month storage. There was non-significant difference observed from 3 months and slightly significant
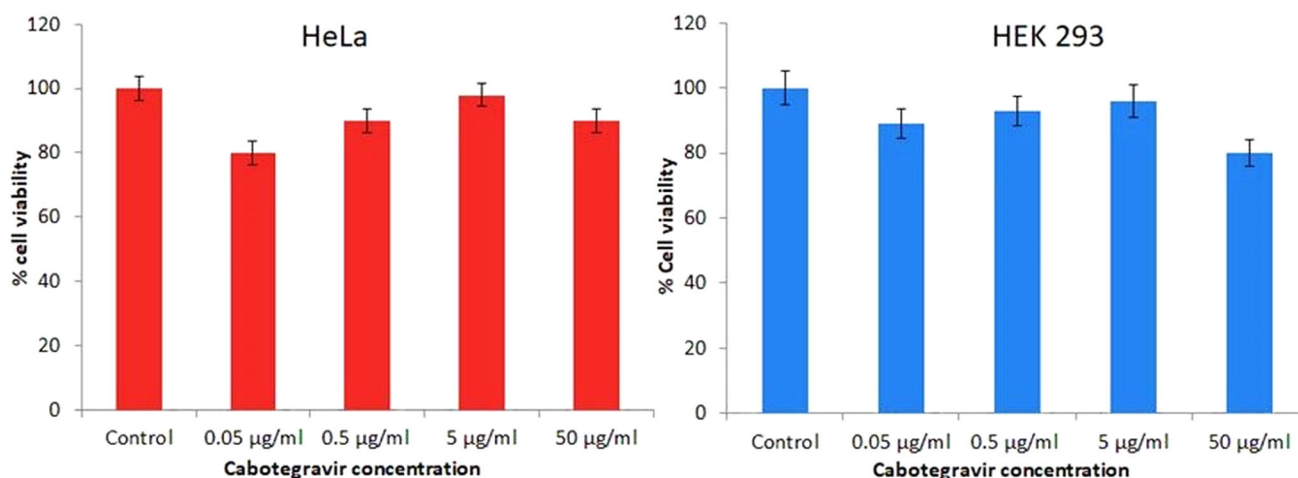
Fig. 7 Cytotoxicity data of CAB gold nanoparticles (GLN-7) on HeLa and HEK 293 cells. Each study performed in triplicate and data shown as mean ± SD

(p < 0.05) from the initial time point. The high reduction in encapsulation efficiency was not found due to the complete entrapment of CAB in the prepared gold NPs. The presence of pectin also prevents the leaching of drug from the NPs.

Conclusions

The present research work was designed to prepare CAB loaded gold nanoparticles. The formulations were optimized using Box Behnken design. The prepared CAB gold nanoparticles (GLN-7) showed a narrow particle size, higher encapsulation efficiency and pH-dependent release behaviour. SEM and TEM study result depicted smooth surface morphology. GLN-7 showed better antimicrobial activity against Gram-positive (*E. coli*) and Gram-negative (*S. aureus*) bacteria. The cell viability study result revealed that the CAB gold nanoparticles (GLN-7) treated HeLa and HEK-293 cells does not exhibited any cytotoxicity. The findings of this study have to be seen in light of some limitations. Thus further in vivo studies investigating the efficacy of the nanoparticles in enhancing oral bioavailability of CAB are required to advocate these findings and future applications.

Declarations

Conflict of interest None.

References

1. UNAIDS, Fact Sheet - Latest Global and Regional Statistics on the Status of the AIDS Epidemic, https://www.unaids.org/en/resources/documents/2021/UNAIDS_FactSheet (2021).
2. UNAIDS, UNAIDS Global AIDS Update-Confronting inequalities-Lessons for pandemic responses from 40 years of AIDS, https://www.unaids.org/en/resources/documents/2021/2021-global-aids-update(2021).
3. UNAIDS, Prevention Gap Report, Geneva, 2016. http://www.unaids.org/sites/ default/files/media_asset/2016-prevention-gap-report_en.pdf.
4. E. Ojewole, I. Mackraj, P. Naidoo, and T. Govende (2008). *Eur. J. Pharm. Biopharm.* **70**, 697.
5. Jose das Neves (2010). MM Amiji, Maria Fernanda Bahia, Bruno Sarmento. *Adv. Drug Deliv. Rev.* **62**, 458.
6. M. S. Cohen, N. Hellmann, J. A. Levy, K. DeCock, and J. Lange (2008). *J. Clin. Invest.* **118**, 1244.
7. J. A. Levy (2009). *AIDS.* **23**, 147.
8. J. A. Levy, *HIV and the Pathogenesis of AIDS*, 3rd ed. (American Society of Microbiology Press, Washington, DC, 2007), p. 644.
9. M. M. Thomson and R. Najera (2005). *AIDS Rev.* **7**, 210.
10. S. Kota, A. W. Khan, S. H. Ansari, R. K. Sharma, and J. Ali (2014). *Int. J. Pharm.* **462**, 129.
11. J. B. Dumond (2007). RF Yeh,. KB Patterson, AH Corbett, BH Jung, NL Rezk, AS Bridges, PW Stewart, MS Cohen, AD Kashuba, *AIDS* **21**, 1899.
12. C. Dobard, N. Makarova, K. Nishiura, et al. (2020). *J. Infect Dis.* **222**, 391.
13. M. Markowitz, I. Frank, G. M. Grant, et al. (2017). *Lancet HIV.* **4**, 331.
14. R. J. Landovitz, S. Li, B. Grinsztejn, et al. (2018). *PLoS Med.* **15**, 1002690.
15. T. Zhoua, H. Su, P. Dash, Z. Lina, B. L. D. Shetty, T. Kocher, A. Szlachetk, B. Lamberty, H. S. Fox, L. Poluektova, S. Gorantla, J. McMillan, N. Gautam, R. L. Mosley, Y. A. B. Edagwa, and H. E. Gendelman (2018). *Biomaterials* **151**, 53.
16. G. D. Bowers, A. Culp, M. J. Reese, G. Tabolt, L. Moss, S. Piscitelli, P. Huynh, D. Wagner, S. L. Ford, and E. P. Gould, Rennan Pan, Yu Lou, DA Margolis, WR Spreen (2015). *Xenobiotica* **25**, 1.
17. W. R. Spreen, S. Min, S. L. Ford, et al. (2013). *HIV Clin. Trials.* **14**, 192.
18. P. K. Jain, K. S. Lee, I. H. El-Sayed, and M. A. El-Sayed (2006). *J. Phys. Chem. B* **110**, 7238.
19. M. R. Groseclose, Stephen Castellino (2019). *Int. J. Mass Spectrom.* **437**, 92.
20. P. Fernanda, P. Faudoa, A. Sizovsa, N. Di Trania, J. Paez-Mayorga, G. Bruno, J. Rhudy, M. Manohar, K. Gwenden, C. Martini, C. Ying, X. Chua, G. Varchi, M. A. Marzinke, and A. Grattoni (2019). *J. Controll. Release* **306**, 89.
21. F. Masse, P. Desjardins, M. Ouellette, and C. Couture, Mahmoud Mohamed Omar, Vincent Pernet, Sylvain Guérin, Elodie Boisselier (2019) *Molecules* **24**, 2929.
22. J. Turkevich, P. C. Stevenson, and J. Hillier (1951). *Discus. Faraday Soc.* **11**, 55.
23. I. Capek (2017). *Adv. Colloid Interface Sci.* **249**, 386.
24. S. D. Mahajan, R. Aalinkeel, W. C. Law, J. L. Reynolds, B. B. Nair, D. E. Sykes, K. T. Yong, I. Roy, P. N. Prasad, and S. A. Schwartz (2012). *Int. J. Nanomed.* **7**, 5301.
25. A. Z. Nurakhmetova, A. N. Azhkeyeva, A. I. Klassen, and S. G. Tatykhanova (2020). *Polymers* **12**, 2625.
26. K. Rahme, M. T. Nolan, T. Doody, G. P. McGlacken, M. A. Morris, C. O. Driscoll, and J. D. Holmes (2013). *RSC Adv.* **3**, 21016.
27. W. Wang, X. Ding, Q. Xu, J. Wang, L. Wang, and X. Lou (2016). *Colloids Surf. B* **148**, 541.
28. E. Boisselier, A. K. Diallo, L. Salmon, C. Ornelas, J. Ruiz, and D. Astruc (2010). *J. Am. Chem. Soc.* **132**, 2729.
29. P. Mukherjee, R. Bhattacharya, P. Wing, L. Wang, S. Basu, J. A. Nagy, and A. Atala, D. Mukhopadhyay, S Soker (2005). *Clin. Cancer Res.* **11**, 3530.
30. S. L. Venable. Gold: A Cultural Encyclopedia. https://silo.pub/gold-a-culturalencyclopedia.html (2011).
31. L. L. Rouhana, J. A. Jaber, and J. B. Schlenoff (2007). *Langmuir.* **23**, 12799.
32. APZ Stevenson, Bea D Blanco, S Civit, et al. (2012). *Nanoscale Res. Lett.* **7**, 151.
33. S. Elzey and V. G. Grassian (2010). *J. Nanopart. Res.* **12**, 1945.
34. J. Gubicza, JL Labar,Quynh L Manh, et al. (2013). *Mater. Chem. Phys.* **138**, 449.
35. N. E. Izak, A. Huk, B. Reidy, et al. (2015). *RSC Adv* **5**, 84172.
36. W. Abdelwahed, G. Degobert, S. Stainmesse, et al. (2006). *Adv Drug Deliv Rev* **58**, 1688.
37. Y. Zhang, Y. Chen, P. Westerhoff, et al. (2008). *Water Res* **42**, 2204.
38. C. M. Burtt and G. Senanayake (2016). *Hydrometallurgy* **164**, 166.

39. S. Dhar, EM Reddy,A Shiras A, et al. (2008). *Chem. Eur J.* **14**, 10244.
40. D. Pooja, S. Panyaram, H. Kulhari, et al. (2014). *Carbohydr. Polym.* **110**, 1.
41. H. M. Joshi, D. R. Bhumkar, K. Joshi, et al. (2006). *Langmuir.* **22**, 300.
42. S. Borker, M. Patole, A. Moghe, et al. (2017). *Gold Bull.* **50**, 235.
43. S. Piriyaprasarth and P. Sriamornsak (2011). *Carbohydr. Polym.* **83**, 561.
44. R. K. Mishra, A. K. Banthia, and A. B. A. Majeed (2012). Asian J. Pharm. *Clin. Res.* **5**, 1.
45. R. M. Devendiran, S. K. Chinnaiyan, N. K. Yadav, G. K. Moorthy, G. Ramanathan, S. Singaravelu, U. T. Sivagnanam, and P. T. Perumal (2016). *RSC Adv.* **6**, 29757.
46. V. G. Kumari, S. Asha, and T. Mathavan (2016). JMA Rajan JMA. *J. Phys. Chem. Biophys.* **6**, 398.
47. K Alexander. Dosage forms and their routes of administration. In: Hacker M, Messer W, Bachmann K, editors. Pharmacology: Principles and Practice. Academic Press (2009) 14:9.
48. D. Hodge, D. J. Back, S. Gibbons, S. H. Khoo, and C. Marzolini (2021). *Clin. Pharmacokinet.* **60**, 835.
49. S. Brissos, M. R. Veguilla, D. Taylor, and V. Balanzá-Martinez (2014). *Ther Adv Psychopharmacol.* **4**, 198.
50. US-FDA Publication. FDA Approves Cabenuva and Vocabria for the Treatment of HIV-1 Infection. https://www.fda.gov/drugs/human-immunodeficiency-virus-hiv/fda-approves-cabenuva-and-vocabria-treatment-hiv-1-infection. (2021).
51. S. Rerks-Ngarm, P. Pitisuttithum, S. Nitayaphan, J. Kaewkungwal, J. Chiu, et al. (2009). *N Eng J Med* **361**, 2209.
52. N. A. Moges, G. M. Kassa, and J. A. I. D. S. Clin (2014). *Res.* **5**, 30.
53. B. S. Jaliff, J. Dahl-Knudsen, A. Petersen, R. Skov, and T. Benfield (2014). *BMJ Open.* **4**, e004075.
54. J. Yin, A. C. Collier, A. M. Barr, W. G. Honer, and R. M. Procyshyn (2015). *J. Clin. Psychopharmacol.* **35**, 447.
55. V. O. Chan, J. Colville, T. Persaud, O. Buckley, S. Hamilton, and W. C. Torreggiani (2006). *Eur J. Radiol.* **58**, 480.
56. V. A. Fonner, S. L. Dalglish, C. E. Kennedy, et al. (2016). *AIDS* **30**, 1973.
57. B. Hanscom, H. E. Janes, P. D. Guarino, et al. (2016). *J. Acquir. Immune Defic. Syndr.* **73**, 606.
58. S. D. Mahajan, R. Aalinkeel, W. C. Law, et al. (2012). *Int. J. Nanomed.* **7**, 5301.
59. T. Mamo, E. A. Moseman, N. Kolishetti, et al. (2010). *Nanomedicine.* **5**, 269.
60. J. K. Patra, G. Das, L. F. Fraceto, et al. (2018). *J. Nanobiotechnol.* **16**, 71.
61. Clinical info HIV gov by AIDS Research Advisory Council (OARAC). Guidelines for the Use of Antiretroviral Agents in Adults and Adolescents with HIV. https://clinicalinfo.hiv.gov/sites/default/files/guidelines/documents/AdultandAdolescentGL.pdf (2021).
62. S. Borker, M. Patole, A. Moghe, and V. Pokharkar (2017). *Gold Bull.* **50**, 235.
63. P. Rawat and S. Gupta (2021). *Med. Hypotheses* **150**, 110576.
64. P. Rawat, I. Ahmad, D. Vohora, F. J. Ahmad, and S. Talegaonkar (2015). *J. Pharm. Innov.* **10**, 130.
65. T. Zhou, Z. Lin, P. Puligujja, D. Palandri, J. Hilaire, M. Araínga, N. Smith, N. Gautam, J. McMillan, Y. Alnouti, X. Liu, and B. Edagwa, Howard E Gendelman (2018). *Nanomedicine* **13**, 871.
66. C. G. England and M. C. Miller, Ashani Kuttan, JO Trent, HB Frieboes (2015). *Eur. Jo. Pharm. Biopharm.* **92**, 120.
67. S. Dash, P. N. Murthy, L. Nath, and P. Chowdhury (2010). *Acta Pol. Pharmaceut.* **67**, 217.
68. T. Chaowanachan, E. Krogstad, C. Ball, A. Kim Woodrow (2013). *PLoS ONE* **8**, 61416.
69. K. H. Choa and J. E. Park, Tetsuya Osaka, S. G. Park (2005). *Electrochim. Acta* **51**, 956.
70. ICH Quality Guidelines for Pharmaceutical Stability Storage - Q1 Scientific
71. G. Rajakumar, T. Gomathi, A. A. Rahuman, M. Thiruvengadam, G. Mydhili, S. H. Kim, T. J. Lee II., and M. Chung (2016). *Appl. Sci.* **6**, 222.
72. Y. Yulizar and T. Utari. Harits Atika Ariyanta, Digha Maulina (2017). *J. Nanomater.* **24**, 1.
73. SM Navarro Gallon, E Alpaslan, M Wang, PL Casanova, ME Londono, L Atehortúa, JJ Pavón, TJ Webster (2019). *Mater. Sci Eng. C* **99**, 685.
74. H. Katas and C. S. Lim, Ahmad Yasser Hamdi Nor Azlan, Fhataheya Buang, Mohd Fauzi Mh Busra (2019). *Saudi Pharm. J.* **27**, 283.
75. M. Sandra, Navarro Gallon, Ece Alpaslan, Mian Wang, Phillip Larese-Casanova, ME Londono, Lucía Atehortua, JJ Pavon, TJ Webster (2019). *Mater. Sci. Eng. C* **99**, 685.
76. A. Shibata and E. McMullen, Alex Pham, M Belshan, Bridget Sanford, Y Zhou, Michael Goede, AA Date, J Christopher Destache (2013). *AIDS Res. Hum. Retrovir.* **29**, 746.
77. Halina Krowicka, EJ Robinson, Rebecca Clark, Shannon Hager, Stephanie Broyles, SH Pincus (2008). *Aids Res. Hum. Retrovir.* **24**, 957.
78. J. Reznicek, M. Ceckova, Z. Ptackova, O. Martinec, L. Tupova, L. Cerveny, and F. Staud (2017). *Antimicrob. Agents Chemother.* **61**, 00837.
79. A. Sett, M. Gadewar, P. Sharma, M. Deka, and U. B. Adv (2016). *Nat. Sci.* **7**, 025005.